

Catalyst design for highly efficient base-free carbon dioxide hydrogenation to formic acid

Andreas Weilhard,^a Kevin Salzmann,^b Jairton Dupont,^c Martin Albrecht,^{b*} Victor Sans^{a,d*}

- a) Faculty of Engineering, University of Nottingham, Nottingham, NG7 2RD, UK
- b) Department of Chemistry & Biochemistry, University of Bern, Freiestrasse 3, 3012 Bern, Switzerland
- c) Institute of Chemistry – UFRGS – Av. Bento Gonçalves, 9500 Porto Alegre 91501-970 – RS Brazil
- d) Institute of Advanced Materials (INAM), Universitat Jaume I, 12006, Castellon, Spain

Corresponding author e-mail: sans@uji.es, martin.albrecht@dcb.unibe.ch

Abstract

We report on new ruthenium complexes as catalysts for the efficient transformation of CO₂ into formic acid as a high-value chemical and fuel. Remarkably, these complexes catalyze the hydrogenation of CO₂ selectively and without employing any base, which improves the sustainability of the process when compared the common base-assisted technologies. The molecular catalyst design relies on donor-flexible and synthetically versatile pyridylidene amide (PYA) ligands which allows the ligand architecture to be varied in a controlled manner to gain valuable insights for the improvement of catalyst performance. Modification of the ligand properties directly influence the catalytic process by shifting the turnover limiting step, the reaction mechanism and the stability upon the acidification of the reaction media and provide access to high-performance systems reaching turnover numbers of several thousands and turnover frequencies up to 350 h⁻¹.

Introduction

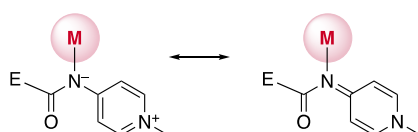
The transformation of carbon dioxide (CO_2) into chemicals and fuels is a key challenge of the 21st century and has gained a lot of interest in recent years.¹⁻² Indeed, the synthesis of commodity chemicals, such as (poly)carbonates, hydrocarbons, methanol, formic acid and specialty chemicals¹ from CO_2 is highly desirable, as CO_2 represents a cheap, and virtually infinite source of C1 building blocks.¹⁻² Except for the case of carbonates, CO_2 has to be reduced to a lower oxidation state. As reduced and synthetically useful product, formic acid (FA) represents formally the easiest target, requiring one dihydrogen molecule to react with one molecule of CO_2 to form FA and reducing formally the oxidation state of carbon from +IV to +II. Indeed the transformation of CO_2 to FA using H_2 *via* artificial photosynthesis has attracted high scientific and economic interest, also because CO_2 reduction is environmentally much more benign compared to the current production of FA by formal water carbonylation³ at a megaton capacity per year.⁴ Furthermore, FA has potential applications as a hydrogen storage vector.⁵⁻⁹

The hydrogenation of CO_2 is thermodynamically and kinetically challenging.² Indeed, the hydrogenation of CO_2 and H_2 in the gas phase yielding FA in liquid phase is entropically highly unfavourable and renders the reaction endergonic.¹⁰⁻¹¹ Most commonly the thermodynamic equilibrium is shifted to the product side by the addition of stoichiometric amounts of base. Under these conditions a plethora of noble metal catalyst formed by various types of ligands such as N-heterocyclic carbenes¹²⁻¹³, half sandwich,^{5, 14-16} pincers¹⁷⁻²⁰ and phosphine²¹⁻²⁵ combined with a broad range of transition metals, including iron,²⁶⁻²⁹ nickel,³⁰⁻³¹ copper and cobalt³⁴⁻³⁶ have shown to be remarkably active ($\text{TON} > 10^6$).¹⁷ The key step in those processes is the formation of formate salts and adducts, which shifts the thermodynamic equilibrium to the product side. This increases the enthalpy and makes the reactions highly exothermic. Nevertheless, this energy has to be overcome during downstream processing to be able to utilize the formate salt synthesized in the presence of stoichiometric amounts of base. Currently, major strategies involve reactive distillation^{10, 37-38} or utilization of scCO_2 ³⁹ as eluent phase to liberate formic acid from the reaction media, which is both economically and

environmentally unattractive due to the energy involved as well as the huge quantities of waste produced.

In a more sustainable fashion, the reaction can be carried out in pure solvents without the addition of base. In this regard DMSO has found increased attention.⁴⁰⁻⁴² Here the basic properties of the solvent are exploited to stabilize the product by hydrogen bonding⁴¹ and can be further enhanced by the addition of small amounts of water.⁴⁰ Furthermore, water⁴³⁻⁴⁵ and ionic liquids (ILs)⁴⁶⁻⁴⁸ have demonstrated to facilitate the formation of FA from CO₂ and H₂. However, in most cases the catalytic turnover⁴¹⁻⁴² and concentrations of FA obtained⁴³⁻⁴⁵ are relatively modest, with TONs<1000. Very recently, we have reported that ionic liquids can efficiently mediate the hydrogenation of CO₂ to formic acid by acting as a buffer.⁴⁶⁻⁴⁷ Indeed, in the presence of ILs the reaction can be carried out in less basic solvents including THF, MeCN and MeTHF,⁴⁷ which are easier to separate than DMSO or water by stripping due to their relatively low boiling point.

In order to improve the catalytic performance and to benefit from the clear advantages of base-free FA synthesis, we designed ruthenium complexes containing an electronically flexible pyridylidene amide (PYA) ligand.⁴⁹⁻⁵¹ These ligands stabilize different electronic configurations at the metal center through unique toggling between a limiting zwitterionic and neutral resonance structure (Scheme 1),⁵²⁻⁵⁴ which is key for efficient redox catalysis.⁵⁵⁻⁵⁷ Here, a set of neutral and cationic ruthenium complexes featuring PYA ligands are demonstrated to be efficient CO₂ reduction catalysts and produce FA in the absence of a base. Kinetic analysis, electrochemistry and spectroscopic analyses offer valuable insights into the catalyst reactivity, stability and activity under buffering conditions and provide structure-activity relationships for the sustainable CO₂ hydrogenation to formic acid.

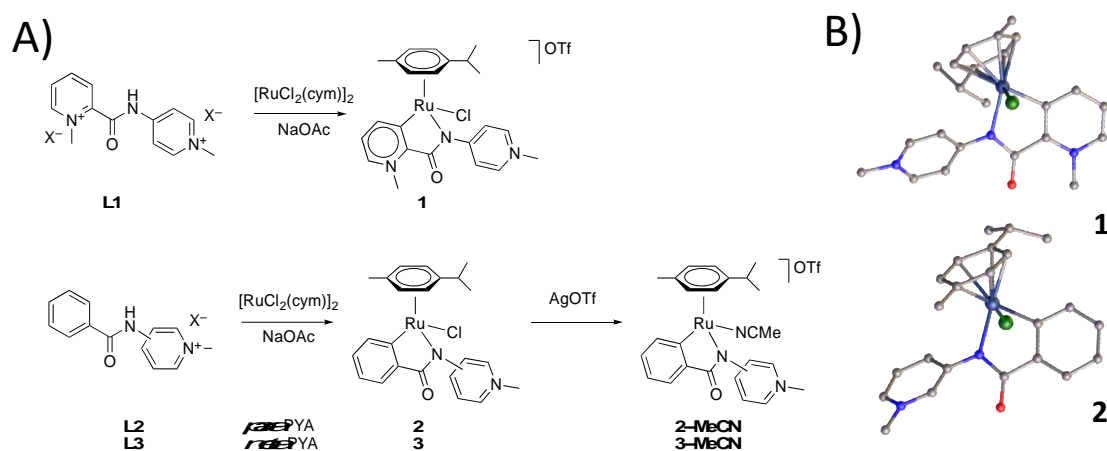


Scheme 1: Limiting resonance structures of PYA ligands featuring a zwitterionic amide (left) for stabilizing electron-poor (high-valent) metal centers, and the formally neutral limiting imine resonance form for stabilizing electron-rich (low-valent) metal centers (right); E may be a (non-)chelating functional group.

Results and discussion

Synthesis of the ruthenium complexes and evaluation of their catalytic activity in CO₂ reduction. Complexes **1–3** were synthesized by reaction of the known pyridinium salts **L1–L3** with [Ru(cym)Cl₂]₂ in the presence of NaOAc (Scheme 2).⁵⁸ This protocol afforded the cationic complex **1** containing a *para*-PYA ligand stabilized by a chelating pyridylidene unit in 61% yield, and the formally neutral complexes **2** and **3** in about 40% yield. These latter complexes were also prepared stepwise from the pyridinium salt by first deprotonating the pyridinium salt to form the free pyridylidene, followed by cycloruthenation. All complexes are air- and moisture-stable solids. Coordination of the PYA ligand site was indicated by the downfield shift of the PYA proton resonances (e.g. from δ = 9.25 (DMSO-*d*₆) in **L3** to 9.86 (CDCl₃) for H α in complex **3**), and the loss of one aromatic signal with concomitant desymmetrization of the remaining resonances established successful cyclometallation, see SI. Further evidence for the formation of complexes **1–3** was obtained from a single crystal X-ray diffraction analysis, which confirmed the anticipated connectivity pattern (Scheme 2). Further details on data collection and refinement parameters are compiled in Tables S1. Crystallographic data for the structure have been deposited with the Cambridge Crystallographic Data Centre (CCDC) as supplementary publication number 19182143098. Complex **1** featuring a pyridylidene NHC ligand and a *para*-PYA ligand was cationic and featured an OTf[–] anion. Notably, the donor properties of the three chelates is reflected in the electron density at the ruthenium center, quantified by cyclic voltammetry and revealing a shift of the Ru^{II}/Ru^{III} oxidation potential from $E_{1/2}$ = +0.83 V (for complex **1** with a formally neutral pyridylidene–PYA chelate) to lower potential for complexes **2** and **3** with an anionic phenyl-PYA chelating ligand ($E_{1/2}$ = +0.52 and +0.46 V vs SCE, all values in MeNO₂). This trend

suggests stronger donor properties of the *meta*-PYA unit compared to the para-PYA analogue, in agreement with previous studies.⁵⁶



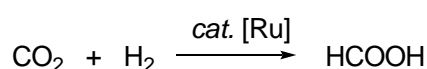
Scheme 2. A) Synthesis of complexes **1–3** and the solvent analogues **2-MeCN** and **3-MeCN**. B) X-ray structures of **1** and **3** (both 50% probability, OTf anion of **1** and all H atoms omitted for clarity)

The neutral complexes **2** and **3** were readily transformed into their cationic species **2-MeCN** and **3-MeCN**, respectively, upon halide abstraction with AgOTf in MeCN (Scheme 2). Formation of the solvent complex is accompanied by an upfield shift of the PYA H α protons and a downfield shift of the PYA H β protons in **2-MeCN** compared to **2**. These shifts are indicative for a larger relevance of the zwitterionic vs the charge-neutral limiting resonance form, in agreement with the lower electron density at the ruthenium center when bound to a MeCN ligand vs an anionic chloride. Interestingly, cyclic voltammetry does not suggest a change of the electronic configuration at the ruthenium center and the Ru^{II}/Ru^{III} redox potential of **2-MeCN** ($E_{1/2} = 0.52$ V vs SCE, MeNO₂ solution) is identical to that of complex **2**, suggesting a very efficient compensation of the lower donor properties of MeCN vs Cl[−] by the more zwitterionic PYA resonance form (see SI for further details).

For an initial evaluation of these complexes in CO₂ reduction catalysis, we chose DMSO:H₂O (19:1 v/v%) as the solvent system in combination with 1-butyl-2,3-dimethylimidazolium acetate (BMMI.OAc) as an additive. Under these conditions, the ionic liquid, BMMI.OAc, acts as a

buffer during the formation of formic acid or the combination of IL and water may also catalyze the formation of carbonates.^{47, 59-61} Further stabilization of the product is imparted by solvent cluster formation by FA, water and DMSO.⁴⁰⁻⁴¹ In the presence of H₂ and CO₂ (P(H₂) = P(CO₂) = 30 bar, T = 70°C), all PYA ruthenium complexes catalyze the formation of FA without the need of an external base (Table 1).

Table 1 Screening of catalytic activity of complexes 1-3-MeCN in the base-free CO₂ hydrogenation to formic acid (FA) ^{a)}



entry	[Ru]	TON ^{b)}	TOF / h ⁻¹ ^{c)}	[FA] / M ^{b)}
1	1	4520±40	117±2.2	1.14±0.01
2	2	2190±40	55±3.6	0.55±0.01
3	3	1930±40	78±2.2	0.49±0.01
4	2-MeCN	1950±40	122±2.3	0.49±0.01
5	3-MeCN	1520±40	50±0.4	0.39±0.01

^{a)} Reaction conditions: 6 mL DMSO:water (5 v/v% water), 3.3 mmol BMML.OAc, 1.52 μmol [Ru] at 70°C, P_{H₂} = P_{CO₂} = 30 bar; ^{b)} determined by ¹H NMR spectroscopy after 72 h using BMML.OAc as an internal standard, average of two independent runs; ^{c)} calculated by linear regression (see SI).

Variation of the ligand scaffold had a pronounced impact on the catalytic activity of the ruthenium complexes. Complex **1** displays a significantly higher catalyst stability than complexes **2**, **3**, **2-MeCN** according to the pertinent TON values, while **3-MeCN** produced the least stable system. The 4520 TONs achieved with complex **1** (Table 1, entry 1) are amongst the highest previously reported catalyst performance under base-free conditions and the final FA concentration of 1.14 M is very close to the predicted thermodynamic limit of FA concentration of 1.2 M under the conditions assayed.^{40-41, 62} In contrast, complexes **2** and **3** achieved much lower FA concentrations around 0.5 M (entries 2–5), suggesting that these

complexes have intrinsic catalytic limitations. While complex **1** is not the only cationic complex in this series, we note that this complex features a formally neutral pyridylidene–PYA ligand scaffold, whereas the other four complexes evaluated here contain a formally anionic phenyl-PYA ligand.

Complexes **1** and **2-MeCN** reach an appreciable maximum turnover frequency (TOF_{max}) around 120 h^{-1} (entries 1,4). Interestingly, complex **2** achieved a significantly lower TOF value ($\text{TOF}_{\text{max}} = 55 \text{ h}^{-1}$) than **2-MeCN** despite the same ligand scaffold. These complexes only differ in their ancillary ligand (Cl vs. MeCN). An inverse effect was observed for complexes **3** and **3-MeCN** (entries 3,5). Modification of the PYA unit from a *para* substituted system in **2** to the more electron-donating *meta* analogue (complex **3**) increases the rate from 55 h^{-1} to 78 h^{-1} , suggesting that electron donating effects are relevant for imparting higher catalytic activity.

These results clearly indicate that both the PYA-ligand and the ancillary ligand play an important role on the catalytic activity. In order to identify the effects determining the rate of catalytic conversion and stability, we investigated a series of parameters such as turnover limiting steps, effect of pressure, and activation energies for this base-free CO_2 hydrogenation process.

Analysis of turnover-limiting steps

In a first approximation, hydrogenation of CO_2 to FA can be divided into two steps. First CO_2 inserts into a metal hydride bond to yield a metal formate complex. In the second step H_2 reacts with this complex to release FA and regenerate the active hydride (Figure 1A). From this simplified mechanism three scenarios can arise: (i) either H_2 activation is the turnover limiting step (TLS) and the rate is solely dependent on the partial pressure of H_2 , or (ii) CO_2 insertion is turnover limiting and thus the rate is dependent only on the partial CO_2 pressure, or (iii) both steps display similar rates and a dependence on both CO_2 and H_2 pressure is

observed. In order to probe the nature of the TLS, we therefore evaluated complexes **1**, **2**, and **3** under varying partial pressures of CO₂ and H₂.

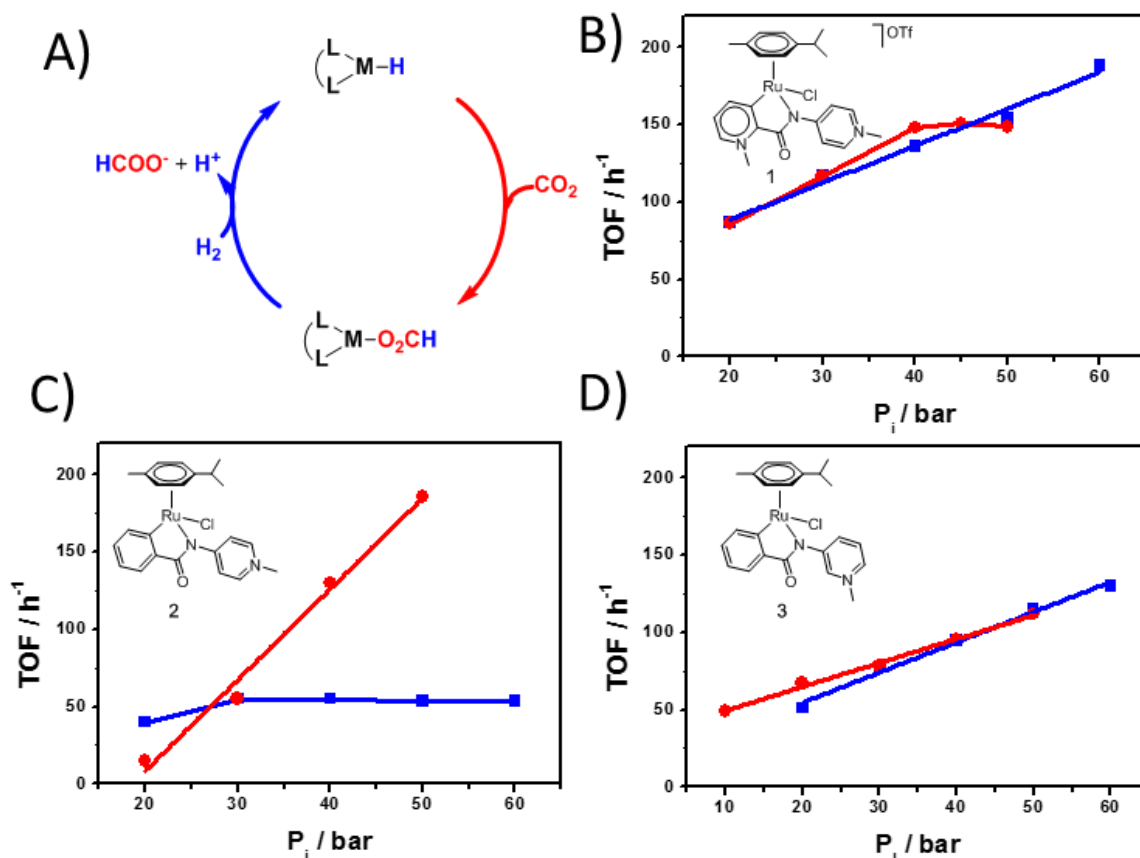


Figure 1 Determination of the turnover limiting step (TLS) for complexes **1**, **2** and **3**. A) Schematic representation of a simplified mechanism of the hydrogenation of CO₂ to FA, divided into two main steps, the insertion of CO₂ (red) and H₂ activation (blue). B)-D) catalytic activity of complexes **1–3** upon variation of the partial pressure P_i of either CO₂ (red) or H₂ (blue), whilst keeping the pressure of the other reactant constant at 30 bar. Reaction conditions: $T = 70^\circ\text{C}$, 6 mL DMSO:H₂O (5 v/v% H₂O), 3.3 mmol BMMI.OAc. and 1.52 μmol of ruthenium complex.

With complex **1**, the catalytic activity is linearly dependent on the partial hydrogen pressure, whilst an increase in partial CO₂ pressure led to a plateau around 150 h⁻¹ when reaching 40 bar CO₂ pressure, clearly indicating that the TLS is associated with the H₂ activation process (Figure 1B). The CO₂ dependence of the rate at low partial pressure of CO₂ has been attributed to the high solubility of H₂ in CO₂, which increases the effective concentration of H₂ in the

reaction media.⁶³⁻⁶⁴ A markedly different behavior was observed for complex **2**, as the rate is essentially independent of the H₂ pressure, yet directly correlates with changes in the partial CO₂ pressure (Figure 1C), identifying CO₂ insertion as the TLS. The pressure-dependence of the catalytic activity of complex **2** is about three times stronger than that of complex **1** (Δ TOF ca. 5.9 h⁻¹ \pm 0.5 h⁻¹ per bar CO₂ for **2** vs 2.4 h⁻¹ \pm 0.2 h⁻¹ per bar H₂ for **1**).

Complex **3** showed a more complex behavior, with a linear dependence on both H₂ and CO₂ insertion (Figure 1D), suggesting that both steps are energetically closely related. Such a models are supported by catalytic runs for which the total pressure was kept constant at 60 bar, yet the partial pressures were varied (Figure 2). The rate is almost unaffected in this regime. The weakly positive dependence on H₂ pressure points to H₂ activation as the slightly more energetic and hence turnover-limiting step rather than CO₂ insertion.

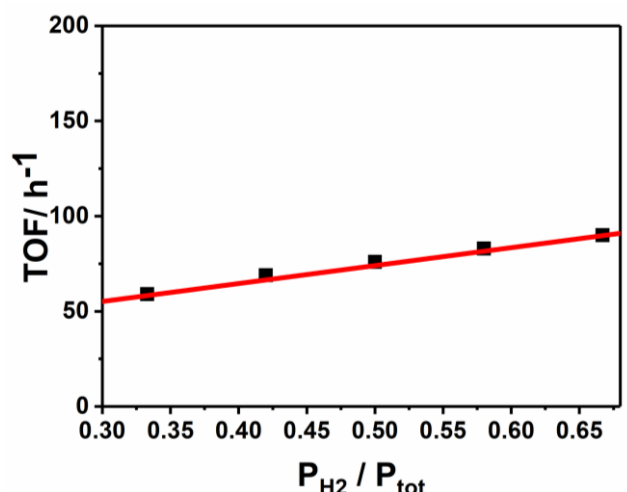


Figure 2. Effect of gas composition on TOF for complex **3** by variation of gas composition at a constant total pressure (60 bar) with 1.52 μ mol complex **3** and 3.3 mmol BMMI.OAc at 70°C in 6 mL DMSO:H₂O (5 v/v% H₂O).

Interestingly, a change in the TLS as observed for complexes **1** and **2** has not been reported for Ru(II) complexes, even though computational studies have predicted that the activation for CO₂ and H₂ are energetically close for Ru(II)-catalysts.⁶⁵ Calculations on the thermodynamics of the hydrogenation process do not identify any one step to be particularly facile, and

therefore the insertion of CO₂ may be endergonic or exergonic.⁶⁶⁻⁶⁷ However, a change in TLS has been reported upon changing the active metal center. With complexes of Co and Ir, CO₂ insertion is rate limiting whilst for Ru and Fe the H₂ activation is generally considered as the limiting step.^{43-44, 65, 68}

Table 2 Optimized catalytic performance of complexes 1–3^{a)}

Entry	[Ru]	P _{H₂} :P _{CO₂} / bar	TON ^{b)}	TOF _{max} / h ⁻¹ ^{b)}	[FA] / M ^{b)}
1	1	60:30	4520±40	188±8	1.15±0.01
2	2	30:50	2010±40	186±15	0.51±0.01
3	3	60:30	1930±40	130±5	0.49±0.01
4	3	30:50	1930±40	115±5	0.49±0.01
5	2-MeCN	30:50	1950±40	340±60 ^{c)}	0.49±0.01

^{a)} Reaction conditions: 6 mL DMSO:water (5 v/v% water) 1.52 μmol [Ru], 3.3 mmol BMML.OAc at 70°C;

^{b)} determined by ¹H NMR spectroscopy after 72 h using BMML.OAc as an internal standard, average of two runs; ^{c)} Determined as maximum TOF calculating the variation of FA concentration as a function of time.

Identification of the TLS for each complex allows for tailoring the reaction conditions to enhance the catalytic performance of each complex. Under optimized conditions, *i.e.* in the presence of an excess of the turnover-limiting component, significantly higher TOF_{max} up to 340±60 h⁻¹ are accessible (Table 2), even though the TON does not significantly change compared to the original conditions studied (*cf* Table 1). This observation indicates that the catalytically active species remain unchanged, even though considerably differing reaction conditions are applied.

The variable catalytic activity and the distinct turnover-limiting steps provide evidence that the nature of the ligand plays a significant role in the hydrogenation of CO₂ to FA. Even relatively small modifications in the PYA ligand architecture lead to significant changes in the TLS. For example, with **1** containing a chelating pyridylidene unit with the PYA donor, the TLS is

associated with H₂ activation, whilst substitution of this formally neutral carbene with an anionic phenyl chelating group as in complexes **2** and **2-MeCN** switches the TLS to CO₂ insertion. With **3**, both these steps are energetically close. Furthermore, the differences of complexes **2** and **3** indicate that the TLS is partially defined by the electron density at the metal center, as the *meta*-PYA unit induces a higher electron density at the metal center compared to the *para*-PYA analogue (see CVs Figure S7 in SI).

Modulation of the ancillary ligand in complex **2** from Cl to MeCN led to a more marked dependence of the catalytic activity on the pressure of CO₂ (Figure 3, (Δ TOF ca. 9.0 h⁻¹ per bar CO₂). The stronger dependence is relevant because the TLS for both complexes is the insertion of CO₂. An increase of the partial CO₂ pressure up to 50 bar therefore leads to an outstanding TOF_{max} = 340 h⁻¹ for complex **2-MeCN**. This complex is therefore the most active one of the series investigated here, and also one of the best reported to date for the base-free hydrogenation of CO₂ to FA. Higher rates are only observed under significantly higher pressures⁴⁰ or temperatures,, and only at very early stages, *i.e.* at very low concentrations of FA.⁶⁹

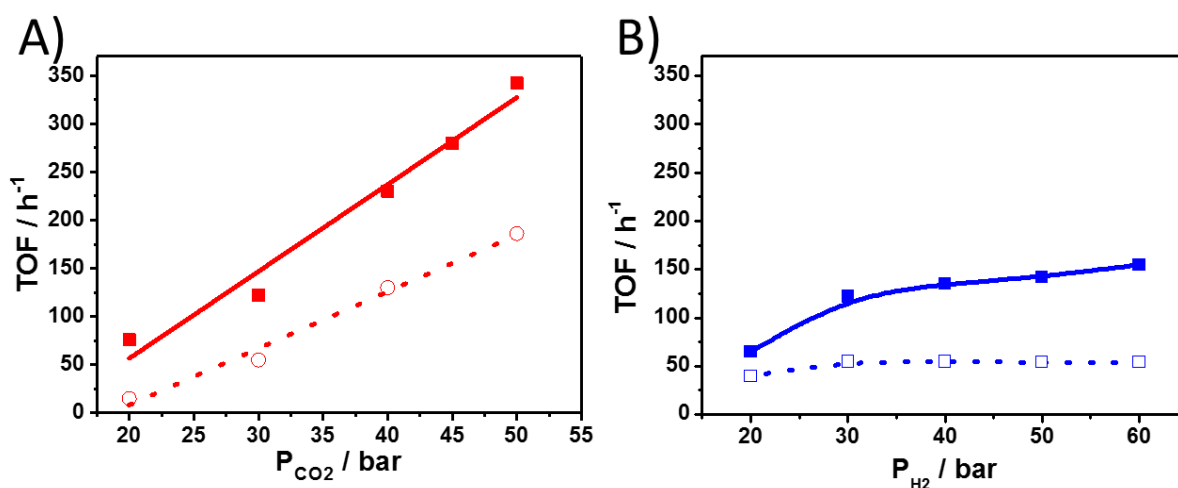


Figure 3. Comparison of catalytic activity of **2** (dotted) and **2-MeCN** (solid) upon A) variation of partial CO₂ pressures (red) ($P(\text{H}_2) = 30$ bar); and B) upon variation of the partial H₂ pressures (blue) ($P(\text{CO}_2) = 30$ bar); General conditions: 1.52 μmol [Ru], 6 mL DMSO:H₂O (5 v/v% H₂O), 3.3 mmol BMMI.OAc, 70°C.

Complex **2-MeCN** showed only small rate increases from 122 h⁻¹ to 150 h⁻¹ when the partial H₂ pressure was increased from 30 to 60 bar (Figure 3B), while complex **2** is completely insensitive to higher H₂ pressure (*cf* Figure 1C). The increasing rate at higher H₂ pressures with **2-MeCN** may be due to an increased concentration of reactant, favourable formation of the active hydride or alternatively a consequence of the higher overall physical pressure. In order to distinguish these effects, complexes **2** and **2-MeCN** were investigated at higher pressure entailed by Ar as an inert gas.

Table 3 Effect of pressure on catalytic performance of **2** and **2-MeCN** ^{a)}

Entry	Complex	T / °C	Ar / bar	[FA] / M	TON	TOF / h ⁻¹	ΔV^\ddagger / M ⁻¹ ^{b)}
1	2	90	50	0.175 ± 0.01	695 ± 42	34.5 ± 3	≥ 0
2	2	90	-	0.195 ± 0.01	749 ± 42	37.5 ± 3	-
3	2-MeCN	80	50	0.185 ± 0.01	695 ± 42	37.5 ± 3	< 0
4	2-MeCN	80	-	0.14 ± 0.01	564 ± 42	31 ± 3	-

^{a)} Reaction conditions: P_{CO_2} = 20 bar, P_{H_2} = 10 bar, 6 mL DMSO:water (5 v/v% water), 3.3 mmol BMMI.OAc, 1.52 μmol [Ru], 20 h, average of 2 runs; ^{b)} sign of ΔV^\ddagger estimated from ΔTOF between catalytic runs with and without Ar.

The addition of 50 bar of argon to the catalytic system based on complex **2** did not lead to any significant change in rate of catalytic CO₂ hydrogenation (Table 3, entry 1 vs 2). In contrast, a 20% increase of the TOF was observed when **2-MeCN** was used as the catalyst precursor (entry 3 vs 4). The increased rate noted for **2-MeCN** indicates a negative volume of activation according to Eq. 1 in the SI.

This negative value of ΔV^\ddagger suggests an associative process for **2-MeCN** in the TLS, while the TLS for the hydrogenation with complex **2** is volume-neutral. Two predominant mechanisms for the CO₂ insertion have been discussed which depend on the nucleophilicity and sterics around the metal center. Hence, strong nucleophiles such as metal amines, and metal

hydrides with low steric demand generally proceed through a so-called inner sphere mechanism, involving coordination of CO₂ to the metal center and simultaneous hydride transfer to the CO₂ in a concerted, associative fashion.⁷⁰⁻⁷¹ With most metal hydrides and other weaker nucleophiles, an outer sphere mechanism is prevalent, consisting of an initial hydride transfer to CO₂ and formation of a zwitterionic intermediate comprised of a positively charged metal center and a formate anion. In a second step this zwitterionic intermediate rearranges to the formate complex (*cf.* Figure 1A).⁷⁰⁻⁷¹ According to this model, the negative volume of activation implies a concerted associative TLS for the **2-MeCN**-catalyzed process, whilst with **2** the outer sphere mechanism with no significant volume change is dominant. Moreover, these data suggest that the ruthenium-hydride intermediate derived from **2-MeCN** has a lower steric demand or is a stronger nucleophile than the one derived from **2**. It has been shown that the inner sphere mechanism proceeds faster than the outer sphere mechanism,⁷¹ in agreement with the twice higher rate of CO₂ hydrogenation observed with **2-MeCN** compared to **2** (340 vs 186 h⁻¹, *cf.* Table 2).

Ligand electronic effects on catalytic activity

The catalytic implications of varying electronic effects of the different PYA ligand scaffolds in complexes **1–3** has been quantified by determining the activation energy for CO₂ hydrogenation with each complex. An Arrhenius plot from rate measurements in the 60–90 °C temperature range is linear (Figure 3) and provides the activation energies (*E_a*) and pre-exponential factors (*ln A*) for the complexes (Table 4). To further probe the electronic flexibility of the PYA ligand, the activation energy for complex **2** was also determined in THF as a less polar solvent than DMSO. Lower polarity solvents were previously shown to favour the neutral PYA resonance structure more than the zwitterionic one (*cf.* Scheme 1),⁵²⁻⁵⁴ which is also reflected in the higher Ru^{II}/Ru^{III} oxidation potential of complex **2** in THF than in polar solvents (*E*_{1/2} = +0.63 V vs +0.52 V in MeNO₂ as proxy for DMSO). Activation energies in THF as the main solvent were measured in the presence of 1-decyl-2,3-dimethylimidazolium acetate (C₁₀MMI.OAc) rather than BMMI.OAc as IL media.

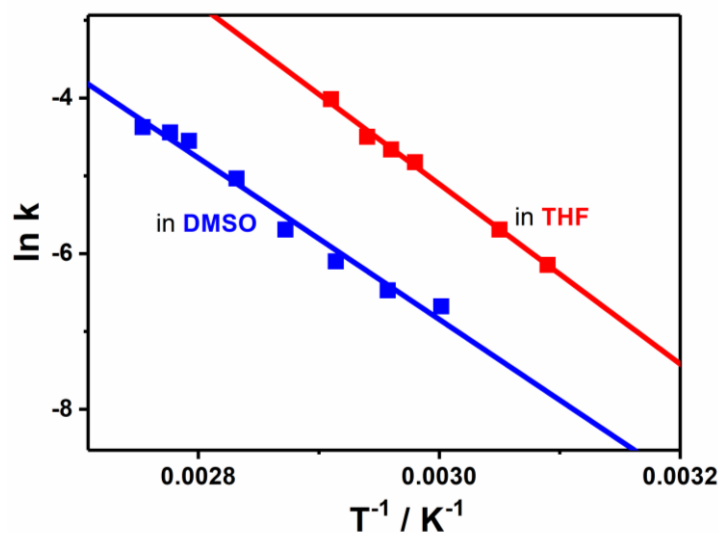


Figure 4 Arrhenius plot of **2** in DMSO:water with 3.3 mmol BMMI.OAc (blue), and in THF:water with 3.3 mmol C₁₀MMI.OAc (red) using 8 μ mol catalyst and $P_{\text{CO}_2} = P_{\text{H}_2} = 20$ bar.

Complex **2** in polar and apolar media and complex **3** showed a direct correlation between the activation energy and the energy donation ability of the ligands. When compared to the *para*-PYA ligand system in complex **2** ($\Delta E_a = 86$ kJ mol⁻¹; Table 4, entry 2), the *meta*-PYA ligand of complex **3** is stronger donating, which is also shown by the 60 mV easier Ru^{II/III} oxidation. This increased electron density lowers the activation energy by 15 kJ mol⁻¹ (entry 3). In contrast, the larger contribution of the neutral resonance structure of the *para*-PYA ligand in THF lowers the electron density at ruthenium (110 mV higher oxidation potential) which also imparts a 10 kJ mol⁻¹ higher activation energy compared to the same complex in more polar DMSO solvent (entry 4). This observation suggests a relationship between the hydricity of the critical ruthenium hydride intermediate and the catalytic activity, as established previously for a wide range of catalysts. The hydricity has been shown to directly correlate with the electron density at the metal center, hence allowing to estimate the hydride transfer capability of metal complexes and to compare it to the hydride donor-ability of formate/formic acid.^{30, 34-36, 66, 72-77} In general, higher hydride transfer capabilities lead to higher catalytic activities in the hydrogenation of CO₂. A relationship in between the oxidation potential and the catalytic activity has been established previously with other Ru-catalysts in the hydrogenation of CO₂ under basic conditions.⁷⁸

Table 4 Comparison of the redox potential, Arrhenius activation parameters ^{a)}

Entry	Complex	Solvent	Ionic liquid	$\Delta E_a /$ kJ mol ⁻¹	lnA	E _{1/2} / V
1	1	DMSO:water	BMMI.OAc	62 ± 4.2	18 ± 1.5	0.83
2	2	DMSO:water	BMMI.OAc	86 ± 5.1	24 ± 1.8	0.52
3	3	DMSO:water	BMMI.OAc	71 ± 4.5	19 ± 1.6	0.46
4	2	THF:water	C ₁₀ MMI.OAc	96 ± 3.1	30 ± 1.1	0.63

^{a)} Reaction conditions: 6 mL solvent with 5 v/v% H₂O, 3.3 mmol IL and $P(H_2) = P(CO_2) = 20$ bar and 8 μ mol catalyst.

While complex **2** and **3** follow the expected trend, complex **1** shows a distinct behavior and features the lowest activation energy ($\Delta E_a = 62$ kJ mol⁻¹) despite having the lowest electron density at ruthenium according to cyclic voltammetry (entry 1). Furthermore, complex **1** generated a much higher concentration of FA and TONs were much higher than those of complexes **2** and **3**. These data indicate fundamental differences in the active species derived from **1** compared to those of **2** and **3**, suggesting a distinct reaction mechanism for complex **1**. This difference has been attributed to a beneficial effect of the overall neutral carbene donor ligand pyridylidene-PYA donor ligand in complex **1**, which imparts higher robustness of the catalytically active species than the anionic phenyl-PYA chelates in complexes **2** and **3**. Moreover, this neutral ligand entails less electron density at the ruthenium center of complex **1** compared to that of **2** and **3** (Figure 4B), which implies a less nucleophilic metal hydride for the catalysts derived from **1**. Accordingly, the catalytic hydride intermediate is more resistant to protonation and formation of the inactive ruthenium dihydrogen complex (Figure 4A). This catalyst passivation through protonation is particularly relevant for highly nucleophilic metal hydride species as well as in the high turnover regime, where larger quantities of FA product impart increasingly more acidic conditions. Hence, the higher resistance to acidification of the hydride originating from complex **1** results in higher TON and FA concentrations compared to the performance of complexes **2** and **3** (Figure 4B).

The gas uptake kinetics for complexes **1–3** supported this hypothesis. An exponential decay, which fits very well with first order kinetics was observed for complex **1**, while the uptake curve with complexes **2** and **3** strongly deviate from an exponential fit (Figure 4C). This indicates that complexes **2** and **3** are deactivated before they reach the thermodynamic equilibrium. It is well established that one major deactivation path during the hydrogenation of CO₂ to FA involves the protonation of the active hydride species,⁴⁰ though with complexes **2** and **3**, deactivation may also involve protonation of the phenyl ligand due to the increased acidity, and subsequent ligand dissociation. Irrespective of the exact deactivation mechanism for those complexes, the results obtained here indicate that complex **1** represent an attractive lead complex to develop new high-turnover catalysts for the hydrogenation of CO₂ to FA under base-free conditions.

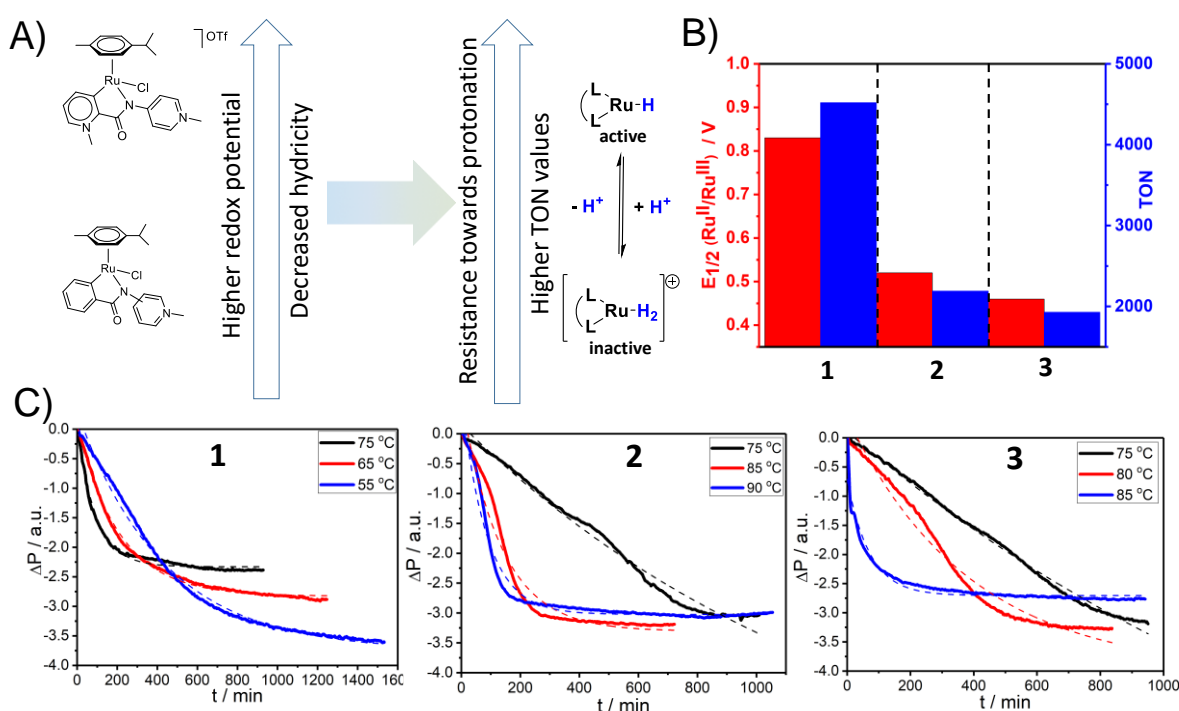


Figure 4. A) Correlation between hydricity and catalyst robustness against acidification of the crucial ruthenium hydride intermediate. B) Correlation between redox potentials $E_{1/2} (Ru(II)/Ru(III))$ values of complexes **1–3** in MeNO₂ as proxy for DMSO and the corresponding TON of the corresponding catalysts (Experimental conditions can be found in table 1). (C) Gas uptake kinetics for complexes **1–3**, solid lines represent experimental data obtained at $P_{H_2} = P_{CO_2} = 20$ bar in 6 mL DMSO:H₂O

and 3.3 mmol BMMI.OAc with 8 μ mol catalyst and dashed lines the best fit to an exponential decay function. Complex **1** shows a different behavior as gas uptake, fits an exponential decay, but not complexes **2** and **3**.

Conclusions

The base-free catalytic hydrogenation of CO₂ to form FA has a number of technical advantages and represents a more sustainable approach compared to the established base-assisted procedures. Direct hydrogenation has inherently a very high atom economy and therefore represents a sustainable alternative to generate chemicals and fuels from CO₂. Specific variation of the ligands bound to the catalytically active ruthenium center provided relevant insights into the mechanism of the reaction and the factors that influence the catalyst performance in terms of TON and TOF. Fine-tuning of the electron density at the metal center is key for catalyst efficiency, with a dual effect observed: high-electron density facilitates CO₂ bonding and increases TOF, even though it also enhances the hydricity of the critical ruthenium hydride intermediate, which favours catalyst protonation due to the increasing acidity of the medium due to the formation of FA. Hence, while high electron density at the metal is beneficial for TOF optimization, low electron density favours the hydride-dihydrogen equilibrium to the catalytically active hydride side, thus enabling high TON values. This ambivalence of electron density emphasizes the relevance of fine-tuning the electronic configuration of the metal center. Moreover, the type of chelating PYA ligand has a direct influence on the nature of the TLS and depending on the set of ligands, either H₂ addition or CO₂ insertion have been observed as limiting step. Likewise, the ancillary ligand (Cl⁻ vs MeCN) modulates the mechanism of CO₂ insertion from inner to outer sphere.

Most interestingly, the catalyst precursor comprised of a formally neutral pyridylidene-PYA ligand showed unique activity. Specifically, the hydricity is markedly reduced and the catalytically active ruthenium hydride species stabilized, which prevents protonation even in the acidic product solution. As a consequence, these complex features results in high turnover

frequency and also a two-fold increase in TON compared to the other complexes, hence representing an attractive lead for further catalyst development.

Acknowledgements

Dr Christof Jaeger is gratefully acknowledged for insightful discussions. The Faculty of Engineering from the University of Nottingham, the Generalitat Valenciana (CIDEAGENT 2018/36), the European Research Council (CoG 615653) and the Swiss National Science Foundation (200020_182663) are gratefully acknowledged for funding.

References

1. Klankermayer, J.; Wesselbaum, S.; Beydoun, K.; Leitner, W., Selective Catalytic Synthesis Using the Combination of Carbon Dioxide and Hydrogen: Catalytic Chess at the Interface of Energy and Chemistry. *Angew. Chem. Int. Ed.* **2016**, *55* (26), 7296-7343.
2. Sordakis, K.; Tang, C.; Vogt, L. K.; Junge, H.; Dyson, P. J.; Beller, M.; Laurenczy, G., Homogeneous Catalysis for Sustainable Hydrogen Storage in Formic Acid and Alcohols. *Chem. Rev.* **2018**, *118* (2), 372-433.
3. Reutemann, W.; Kieczka, H., Formic Acid. In *Ullmann's Encyclopedia of Industrial Chemistry*, Wiley-VCH Verlag GmbH & Co. KGaA: 2000.
4. Mac Dowell, N.; Fennell, P. S.; Shah, N.; Maitland, G. C., The role of CO₂ capture and utilization in mitigating climate change. *Nat. Clim. Chang.* **2017**, *7*, 243-249.
5. Hull, J. F.; Himeda, Y.; Wang, W.-H.; Hashiguchi, B.; Periana, R.; Szalda, D. J.; Muckerman, J. T.; Fujita, E., Reversible hydrogen storage using CO₂ and a proton-switchable

iridium catalyst in aqueous media under mild temperatures and pressures. *Nat. Chem.* **2012**, 4 (5), 383-388.

6. Loges, B.; Boddien, A.; Gärtner, F.; Junge, H.; Beller, M., Catalytic Generation of Hydrogen from Formic acid and its Derivatives: Useful Hydrogen Storage Materials. *Topics Catal.* **2010**, 53 (13), 902-914.

7. Grasemann, M.; Laurenczy, G., Formic acid as a hydrogen source - recent developments and future trends. *Energy Environ. Sci.* **2012**, 5 (8), 8171-8181.

8. Loges, B.; Boddien, A.; Junge, H.; Beller, M., Controlled Generation of Hydrogen from Formic Acid Amine Adducts at Room Temperature and Application in H₂/O₂ Fuel Cells. *Angew. Chem. Int. Ed.* **2008**, 47 (21), 3962-3965.

9. Johnson, T. C.; Morris, D. J.; Wills, M., Hydrogen generation from formic acid and alcohols using homogeneous catalysts. *Chem. Soc. Rev.* **2010**, 39 (1), 81-88.

10. Schaub, T.; Paciello, R. A., A Process for the Synthesis of Formic Acid by CO₂ Hydrogenation: Thermodynamic Aspects and the Role of CO. *Angew. Chem. Int. Ed.* **2011**, 50 (32), 7278-7282.

11. Leitner, W., Carbon Dioxide as a Raw Material: The Synthesis of Formic Acid and Its Derivatives from CO₂. *Angew. Chem. Int. Ed. Eng.* **1995**, 34 (20), 2207-2221.

12. Azua, A.; Sanz, S.; Peris, E., Water-Soluble Ir(III) N-Heterocyclic Carbene Based Catalysts for the Reduction of CO₂ to Formate by Transfer Hydrogenation and the Deuteration of Aryl Amines in Water. *Chem. Eur. J.* **2011**, 17 (14), 3963-3967.

13. Sanz, S.; Azua, A.; Peris, E., '[η⁶-arene)Ru(bis-NHC)]' complexes for the reduction of CO₂ to formate with hydrogen and by transfer hydrogenation with iPrOH. *Dalton Trans.* **2010**, 39 (27), 6339-6343.

14. Wang, W.-H.; Hull, J. F.; Muckerman, J. T.; Fujita, E.; Himeda, Y., Second-coordination-sphere and electronic effects enhance iridium(iii)-catalyzed homogeneous hydrogenation of carbon dioxide in water near ambient temperature and pressure. *Energy Environ. Sci.* **2012**, 5 (7), 7923-7926.
15. Himeda, Y.; Onozawa-Komatsuzaki, N.; Sugihara, H.; Kasuga, K., Simultaneous Tuning of Activity and Water Solubility of Complex Catalysts by Acid–Base Equilibrium of Ligands for Conversion of Carbon Dioxide. *Organometallics* **2007**, 26 (3), 702-712.
16. Himeda, Y.; Miyazawa, S.; Hirose, T., Interconversion between Formic Acid and H₂/CO₂ using Rhodium and Ruthenium Catalysts for CO₂ Fixation and H₂ Storage. *ChemSusChem* **2011**, 4 (4), 487-493.
17. Tanaka, R.; Yamashita, M.; Nozaki, K., Catalytic Hydrogenation of Carbon Dioxide Using Ir(III)–Pincer Complexes. *J. Am. Chem. Soc.* **2009**, 131 (40), 14168-14169.
18. Filonenko, G. A.; Hensen, E. J. M.; Pidko, E. A., Mechanism of CO₂ hydrogenation to formates by homogeneous Ru-PNP pincer catalyst: from a theoretical description to performance optimization. *Catal. Sci. Technol.* **2014**, 4 (10), 3474-3485.
19. Filonenko, G. A.; Smykowski, D.; Szyja, B. M.; Li, G.; Szczygieł, J.; Hensen, E. J. M.; Pidko, E. A., Catalytic Hydrogenation of CO₂ to Formates by a Lutidine-Derived Ru–CNC Pincer Complex: Theoretical Insight into the Unrealized Potential. *ACS Catal.* **2015**, 5 (2), 1145-1154.
20. Filonenko, G. A.; van Putten, R.; Schulpen, E. N.; Hensen, E. J. M.; Pidko, E. A., Highly Efficient Reversible Hydrogenation of Carbon Dioxide to Formates Using a Ruthenium PNP-Pincer Catalyst. *ChemCatChem* **2014**, 6 (6), 1526-1530.

21. Inoue, Y.; Izumida, H.; Sasaki, Y.; Hashimoto, H., CATALYTIC FIXATION OF CARBON DIOXIDE TO FORMIC ACID BY TRANSITION-METAL COMPLEXES UNDER MILD CONDITIONS. *Chem. Lett.* **1976**, 5 (8), 863-864.
22. Tsai, J. C.; Nicholas, K. M., Rhodium-catalyzed hydrogenation of carbon dioxide to formic acid. *J. Am. Chem. Soc.* **1992**, 114 (13), 5117-5124.
23. Fornika, R.; Gorls, H.; Seemann, B.; Leitner, W., Complexes [(P2)Rh(hfacac)](P2= bidentate chelating phosphane, hfacac = hexafluoroacetylacetonate) as catalysts for CO₂ hydrogenation: correlations between solid state structures, ¹⁰³Rh NMR shifts and catalytic activities. *J. Chem. Soc., Chem. Commun.* **1995**, (14), 1479-1481.
24. Graf, E.; Leitner, W., Direct formation of formic acid from carbon dioxide and dihydrogen using the [{Rh(cod)Cl}₂]-Ph₂P(CH₂)₄PPh₂ catalyst system. *J. Chem. Soc., Chem. Commun.* **1992**, (8), 623-624.
25. Elek, J.; Nádasdi, L.; Papp, G.; Laurenczy, G.; Joó, F., Homogeneous hydrogenation of carbon dioxide and bicarbonate in aqueous solution catalyzed by water-soluble ruthenium(II) phosphine complexes. *Applied Catal. A* **2003**, 255 (1), 59-67.
26. Ziebart, C.; Federsel, C.; Anbarasan, P.; Jackstell, R.; Baumann, W.; Spannenberg, A.; Beller, M., Well-Defined Iron Catalyst for Improved Hydrogenation of Carbon Dioxide and Bicarbonate. *J. Am. Chem. Soc.* **2012**, 134 (51), 20701-20704.
27. Robert, L.; Yael, D. P.; Gregory, L.; W., S. L. J.; Yehoshoa, B. D.; David, M., Low-Pressure Hydrogenation of Carbon Dioxide Catalyzed by an Iron Pincer Complex Exhibiting Noble Metal Activity. *Angew. Chem. Int. Ed.* **2011**, 50 (42), 9948-9952.
28. Zell, T.; Milstein, D., Hydrogenation and Dehydrogenation Iron Pincer Catalysts Capable of Metal–Ligand Cooperation by Aromatization/Dearomatization. *Acc. Chem. Res.* **2015**, 48 (7), 1979-1994.

29. Zhang, Y.; MacIntosh, A. D.; Wong, J. L.; Bielinski, E. A.; Williard, P. G.; Mercado, B. Q.; Hazari, N.; Bernskoetter, W. H., Iron catalyzed CO₂ hydrogenation to formate enhanced by Lewis acid co-catalysts. *Chem. Sci.* **2015**, *6* (7), 4291-4299.
30. Burgess, S. A.; Kendall, A. J.; Tyler, D. R.; Linehan, J. C.; Appel, A. M., Hydrogenation of CO₂ in Water Using a Bis(diphosphine) Ni–H Complex. *ACS Catal.* **2017**, *7* (4), 3089-3096.
31. Chakraborty, S.; Zhang, J.; Krause, J. A.; Guan, H., An Efficient Nickel Catalyst for the Reduction of Carbon Dioxide with a Borane. *J. Am. Chem. Soc.* **2010**, *132* (26), 8872-8873.
32. Ryo, W.; Yoshihito, K.; Shin-ichi, H.; Norio, M.; Takao, I., Hydrogenation of Carbon Dioxide to Formate Catalyzed by a Copper/1,8-Diazabicyclo[5.4.0]undec-7-ene System. *Adv. Synth. Catal.* **2015**, *357* (7), 1369-1373.
33. Zall, C. M.; Linehan, J. C.; Appel, A. M., A Molecular Copper Catalyst for Hydrogenation of CO₂ to Formate. *ACS Catal.* **2015**, *5* (9), 5301-5305.
34. Burgess, S. A.; Appel, A. M.; Linehan, J. C.; Wiedner, E. S., Changing the Mechanism for CO₂ Hydrogenation Using Solvent-Dependent Thermodynamics. *Angew. Chem. Int. Ed.* **2017**, *56* (47), 15002-15005.
35. Burgess, S. A.; Grubel, K.; Appel, A. M.; Wiedner, E. S.; Linehan, J. C., Hydrogenation of CO₂ at Room Temperature and Low Pressure with a Cobalt Tetrphosphine Catalyst. *Inorg. Chem.* **2017**, *56* (14), 8580-8589.
36. Jeletic, M. S.; Hulley, E. B.; Helm, M. L.; Mock, M. T.; Appel, A. M.; Wiedner, E. S.; Linehan, J. C., Understanding the Relationship Between Kinetics and Thermodynamics in CO₂ Hydrogenation Catalysis. *ACS Catal.* **2017**, *7* (9), 6008-6017.
37. Zhang, Z.; Hu, S.; Song, J.; Li, W.; Yang, G.; Han, B., Hydrogenation of CO₂ to Formic Acid Promoted by a Diamine-Functionalized Ionic Liquid. *ChemSusChem* **2009**, *2* (3), 234-238.

38. Zhang, Z.; Xie, Y.; Li, W.; Hu, S.; Song, J.; Jiang, T.; Han, B., Hydrogenation of Carbon Dioxide is Promoted by a Task-Specific Ionic Liquid. *Angew. Chem. Int. Ed.* **2008**, *47* (6), 1127-1129.
39. Wesselbaum, S.; Hintermair, U.; Leitner, W., Continuous-Flow Hydrogenation of Carbon Dioxide to Pure Formic Acid using an Integrated scCO₂ Process with Immobilized Catalyst and Base. *Angew. Chem.* **2012**, *124* (34), 8713-8716.
40. Rohmann, K.; Kothe, J.; Haenel, M. W.; Englert, U.; Hölscher, M.; Leitner, W., Hydrogenation of CO₂ to Formic Acid with a Highly Active Ruthenium Acridophos Complex in DMSO and DMSO/Water. *Angew. Chem. Int. Ed.* **2016**, *55* (31), 8966-8969.
41. Moret, S.; Dyson, P. J.; Laurenczy, G., Direct synthesis of formic acid from carbon dioxide by hydrogenation in acidic media. *Nature Commun.* **2014**, *5*, 4017.
42. Sahoo, A. R.; Jiang, F.; Bruneau, C.; Sharma, G. V. M.; Suresh, S.; Roisnel, T.; Dorcet, V.; Achard, M., Phosphine-pyridonate ligands containing octahedral ruthenium complexes: access to esters and formic acid. *Catal. Sci. Technol.* **2017**, *7* (16), 3492-3498.
43. Hayashi, H.; Ogo, S.; Fukuzumi, S., Aqueous hydrogenation of carbon dioxide catalysed by water-soluble ruthenium aqua complexes under acidic conditions. *Chem. Commun.* **2004**, (23), 2714-2715.
44. Ogo, S.; Kabe, R.; Hayashi, H.; Harada, R.; Fukuzumi, S., Mechanistic investigation of CO₂ hydrogenation by Ru(II) and Ir(III) aqua complexes under acidic conditions: two catalytic systems differing in the nature of the rate determining step. *Dalton Trans.* **2006**, (39), 4657-4663.
45. Zhao, G.; Joó, F., Free formic acid by hydrogenation of carbon dioxide in sodium formate solutions. *Catal. Commun.* **2011**, *14* (1), 74-76.

46. Qadir, M. I.; Weilhard, A.; Fernandes, J. A.; de Pedro, I.; Vieira, B. J. C.; Waerenborgh, J. C.; Dupont, J., Selective Carbon Dioxide Hydrogenation Driven by Ferromagnetic RuFe Nanoparticles in Ionic Liquids. *ACS Catal.* **2018**, *8* (2), 1621-1627.
47. Weilhard, A.; Qadir, M. I.; Sans, V.; Dupont, J., Selective CO₂ Hydrogenation to Formic Acid with Multifunctional Ionic Liquids. *ACS Catal.* **2018**, *8* (3), 1628-1634.
48. Yasaka, Y.; Wakai, C.; Matubayasi, N.; Nakahara, M., Controlling the Equilibrium of Formic Acid with Hydrogen and Carbon Dioxide Using Ionic Liquid. *J. Phys. Chem. A* **2010**, *114* (10), 3510-3515.
49. Doster, M. E.; Johnson, S. A., Selective C–F Bond Activation of Tetrafluorobenzenes by Nickel(0) with a Nitrogen Donor Analogous to N-Heterocyclic Carbenes. *Angew. Chem. Int. Ed.* **2009**, *48* (12), 2185-2187.
50. Shi, Q.; Thatcher, R. J.; Slattery, J.; Sauari, P. S.; Whitwood, A. C.; McGowan, P. C.; Douthwaite, R. E., Synthesis, Coordination Chemistry and Bonding of Strong N-Donor Ligands Incorporating the 1H-Pyridin-(2E)-Ylidene (PYE) Motif. *Chem. Eur. J.* **2009**, *15* (42), 11346-11360.
51. Boyd, P. D. W.; Wright, L. J.; Zafar, M. N., Extending the Range of Neutral N-Donor Ligands Available for Metal Catalysts: N-[1-Alkylpyridin-4(1H)-ylidene]amides in Palladium-Catalyzed Cross-Coupling Reactions. *Inorg. Chem.* **2011**, *50* (21), 10522-10524.
52. Donnelly, K. F.; Segarra, C.; Shao, L.-X.; Suen, R.; Müller-Bunz, H.; Albrecht, M., Adaptive N-Mesoionic Ligands Anchored to a Triazolylidene for Ruthenium-Mediated (De)Hydrogenation Catalysis. *Organometallics* **2015**, *34* (16), 4076-4084.
53. Leigh, V.; Carleton, D. J.; Olguin, J.; Mueller-Bunz, H.; Wright, L. J.; Albrecht, M., Solvent-Dependent Switch of Ligand Donor Ability and Catalytic Activity of Ruthenium(II)

Complexes Containing Pyridinylidene Amide (PYA) N-Heterocyclic Carbene Hybrid Ligands.

Inorg. Chem. **2014**, *53* (15), 8054-8060.

54. Navarro, M.; Smith, C. A.; Albrecht, M., Enhanced Catalytic Activity of Iridium(III) Complexes by Facile Modification of C,N-Bidentate Chelating Pyridylideneamide Ligands.

Inorg. Chem. **2017**, *56* (19), 11688-11701.

55. Navarro, M.; Li, M.; Müller-Bunz, H.; Bernhard, S.; Albrecht, M., Donor-Flexible Nitrogen Ligands for Efficient Iridium-Catalyzed Water Oxidation Catalysis. *Chem. Eur. J.* **2016**, *22* (20), 6740-6745.

56. Navarro, M.; Smith, C. A.; Li, M.; Bernhard, S.; Albrecht, M., Optimization of Synthetically Versatile Pyridylidene Amide Ligands for Efficient Iridium-Catalyzed Water Oxidation. *Chem. Eur. J.* **2018**, *24* (24), 6386-6398.

57. Melle, P.; Manoharan, Y.; Albrecht, M., Modular Pincer-type Pyridylidene Amide Ruthenium(II) Complexes for Efficient Transfer Hydrogenation Catalysis. *Inorg. Chem.* **2018**, *57* (18), 11761-11774.

58. Navarro, M.; Li, M.; Bernhard, S.; Albrecht, M., A mesoionic nitrogen-donor ligand: structure, iridium coordination, and catalytic effects. *Dalton Trans.* **2018**, *47* (3), 659-662.

59. Simon, N. M.; Zanatta, M.; dos Santos, F. P.; Corvo, M. C.; Cabrita, E. J.; Dupont, J., Carbon Dioxide Capture by Aqueous Ionic Liquid Solutions. *ChemSusChem* **2017**, *10* (24), 4927-4933.

60. Zanatta, M.; Dupont, J.; Wentz, G. N.; dos Santos, F. P., Intermolecular hydrogen bonds in water@IL supramolecular complexes. *Phys. Chem. Chem. Phys.* **2018**, *20* (17), 11608-11614.

61. Zanatta, M.; Girard, A.-L.; Marin, G.; Ebeling, G.; dos Santos, F. P.; Valsecchi, C.; Stassen, H.; Livotto, P. R.; Lewis, W.; Dupont, J., Confined water in imidazolium based ionic

liquids: a supramolecular guest@host complex case. *Phys. Chem. Chem. Phys.* **2016**, *18* (27), 18297-18304.

62. Weilhard, A.; Dupont, J.; Sans V., Carbon dioxide utilisation Vol 2. Berlin, De Gruyter: **2019**, 329-344. DOI: 10.1515/9783110665147-017

63. Hiraga, Y.; Sato, Y.; Smith, R. L., Development of a simple method for predicting CO₂ enhancement of H₂ gas solubility in ionic liquids. *J. Supercrit. Fluid* **2015**, *96*, 162-170.

64. Lopez-Castillo, Z. K.; Aki, S. N. V. K.; Stadtherr, M. A.; Brennecke, J. F., Enhanced Solubility of Hydrogen in CO₂-Expanded Liquids. *Ind. Eng. Chem. Res.* **2008**, *47* (3), 570-576.

65. Mondal, B.; Neese, F.; Ye, S., Control in the Rate-Determining Step Provides a Promising Strategy To Develop New Catalysts for CO₂ Hydrogenation: A Local Pair Natural Orbital Coupled Cluster Theory Study. *Inorg. Chem.* **2015**, *54* (15), 7192-7198.

66. Waldie, K. M.; Ostericher, A. L.; Reineke, M. H.; Sasayama, A. F.; Kubiak, C. P., Hydricity of Transition-Metal Hydrides: Thermodynamic Considerations for CO₂ Reduction. *ACS Catal.* **2018**, *8* (2), 1313-1324.

67. Matsubara, Y.; Fujita, E.; Doherty, M. D.; Muckerman, J. T.; Creutz, C., Thermodynamic and Kinetic Hydricity of Ruthenium(II) Hydride Complexes. *J. Am. Chem. Soc.* **2012**, *134* (38), 15743-15757.

68. Mondal, B.; Neese, F.; Ye, S., Toward Rational Design of 3d Transition Metal Catalysts for CO₂ Hydrogenation Based on Insights into Hydricity-Controlled Rate-Determining Steps. *Inorg. Chem.* **2016**, *55* (11), 5438-5444.

69. Lu, S.-M.; Wang, Z.; Li, J.; Xiao, J.; Li, C., Base-free hydrogenation of CO₂ to formic acid in water with an iridium complex bearing a N,N[prime or minute]-diimine ligand. *Green Chem.* **2016**, *18* (16), 4553-4558.

70. Hazari, N.; Heimann, J. E., Carbon Dioxide Insertion into Group 9 and 10 Metal–Element σ Bonds. *Inorg. Chem.* **2017**, *56* (22), 13655-13678.
71. Heimann, J. E.; Bernskoetter, W. H.; Hazari, N.; Mayer, James M., Acceleration of CO₂ insertion into metal hydrides: ligand, Lewis acid, and solvent effects on reaction kinetics. *Chem. Sci.* **2018**, *9* (32), 6629-6638.
72. Wiedner, E. S.; Chambers, M. B.; Pitman, C. L.; Bullock, R. M.; Miller, A. J. M.; Appel, A. M., Thermodynamic Hydricity of Transition Metal Hydrides. *Chem. Rev.* **2016**, *116* (15), 8655-8692.
73. Galan, B. R.; Schöffel, J.; Linehan, J. C.; Seu, C.; Appel, A. M.; Roberts, J. A. S.; Helm, M. L.; Kilgore, U. J.; Yang, J. Y.; DuBois, D. L.; Kubiak, C. P., Electrocatalytic Oxidation of Formate by [Ni(PR₂NR'₂)₂(CH₃CN)]²⁺ Complexes. *J. Am. Chem. Soc.* **2011**, *133* (32), 12767-12779.
74. Lilio, A. M.; Reineke, M. H.; Moore, C. E.; Rheingold, A. L.; Takase, M. K.; Kubiak, C. P., Incorporation of Pendant Bases into Rh(diphosphine)₂ Complexes: Synthesis, Thermodynamic Studies, And Catalytic CO₂ Hydrogenation Activity of [Rh(P₂N₂)₂]⁺ Complexes. *J. Am. Chem. Soc.* **2015**, *137* (25), 8251-8260.
75. Waldie, K. M.; Brunner, F. M.; Kubiak, C. P., Transition Metal Hydride Catalysts for Sustainable Interconversion of CO₂ and Formate: Thermodynamic and Mechanistic Considerations. *ACS Sustain. Chem. Eng.* **2018**, *6* (5), 6841-6848.
76. Pitman, C. L.; Brereton, K. R.; Miller, A. J. M., Aqueous Hydricity of Late Metal Catalysts as a Continuum Tuned by Ligands and the Medium. *J. Am. Chem. Soc.* **2016**, *138* (7), 2252-2260.

77. Kubas, G., *Metal-dihydrogen and σ -bond coordination: The consummate extension of the Dewar-Chatt-Duncanson model for metal-olefin π bonding*. *J. Organometal. Chem.* **2001**, 635 (1-2), 37-68.
78. Ono, T.; Qu, S.; Gimbert-Suriñach, C.; Johnson, M. A.; Marell, D. J.; Benet-Buchholz, J.; Cramer, C. J.; Llobet, A., Hydrogenative Carbon Dioxide Reduction Catalyzed by Mononuclear Ruthenium Polypyridyl Complexes: Discerning between Electronic and Steric Effects. *ACS Catal.* **2017**, 7 (9), 5932-5940.

TOC

